JOURNAL OF COMPUTATIONAL PHYSICS 70, 295–310 (1987)

A Numerical Simulation of the Transition to Turbulence in a Two-Dimensional Flow

A. FORTIN

Département de Mathématiques Appliquées, Ecole Polytechnique, C. P. 6079, Succursale "A", Montréal H3C 3A7, Canada

AND

M. FORTIN AND J. J. GERVAIS

Département de Mathématiques, Université Laval, Québec G1K 7P4, Canada

Received January 3, 1986; revised June 9, 1986

A numerical simulation of the transition to turbulence is performed using a finite element method. The unsteady Navier–Stokes equations are discretized using a standard Galerkin approximation and a loading strategy for increasing the Reynolds number. The numerical results are then analysed at different Reynolds numbers showing a transition from a steady-state solution to a weakly chaotic one. Phase space diagrams are presented showing the presence of strange attractors. The dimension and Lyapunov's exponents of these attractors are computed and compared with existing results in the literature.

1. INTRODUCTION

Numerical methods in fluid dynamics are reaching a turning point. The reasons for this are multiple and come from two apparently opposite directions, that is, the development of new computers and the development of new theoretical models.

From the hardware point of view, supercomputers on one hand, as well as the widely available mini-computers, have made possible numerical experimentations that were unthinkable a few years ago.

From the theoretical point of view, our qualitative understanding of the behavior of solutions to the Navier–Stokes equations has made huge progress. There is now no question that these equations can be expected to model the complex phenomena associated with transition to turbulence. Bifurcation theory methods, applied to simplified model problems, yield predictions that are amazingly close to real fluid phenomena and lead one to believe that transition to chaos follows some rather generic patterns [1, 2]. However, numerical evidence that these patterns apply to the Navier–Stokes equations is quite rare even if theoretical results have been obtained (see Constantin *et al.* [3]). The reason is that an accurate simulation of a flow problem requires a very large number of degrees of freedom and the long time runs necessary to correctly simulate bifurcation phenomena are rather expensive in computer time.

0021-9991/87 $3.00

In the present paper, we present a simulation of the transition to chaos in a two-dimensional fluid. The example treated was introduced for reasons totally unrelated to a bifurcation study and it was indeed by chance that this study was begun. The initial aim was to simulate the steady-state problem in a geometry relative to the design of a turbomachinery device. It was rapidly obvious that there was a limiting Reynolds number after which our solution algorithm, based on the Newton–Raphson method, was no longer convergent. Although theoretical results show that steady-state solutions of the Navier–Stokes equations exist for all Reynolds numbers (indeed the generic situation is a finite number of solutions, cf. Temam [19]), it is also expected to meet a Hopf bifurcation in the solution of the time-dependent Navier–Stokes problem from both experimental and theoretical considerations.

A careful continuation method could track a steady-state solution beyond a Hopf bifurcation, but a simple incremental loading in Reynolds number could not follow an unstable branch. A time-dependent computation will follow stable branches and become periodic.

Moving to a time-dependent simulation soon confirmed this hypothesis. A Karman vortex street could clearly be seen behind the blades of our turbine, and the solution was clearly periodic. A Fourier analysis further confirmed this and displayed a fundamental frequency and a few harmonics.

From a practical point of view, this established that a time-dependent simulation was indeed necessary. The question remained of knowing what would happen if the Reynolds number was further increased.

Using a computer that fortunately was free at night, we pursued a set of tests slowly increasing the Reynolds number. A period-doubling bifurcation (also called subharmonic bifurcation) then appeared followed by a second one. To our knowledge this was one of the largest systems for which such a phenomena was observed in numerical simulations. Still increasing, one then sees a second independent frequency coming in and finally a continuous spectrum that can be described as chaos.

We now present these results and some estimates of the dimension of the attractor and of Lyapunov's exponents in order to assess the strangeness of the attractor observed. Finally, we shall discuss some questions remaining unanswered as a result of this simulation.

2. Description of the Problem and Its Discretization

Our starting problem was to simulate an incompressible flow in a section of a turbomachine. As a first approximation we used the two-dimensional Navier–Stokes equations,

$$\partial u_i/\partial t - (2/\mathrm{Re})\,\partial/\partial x_j(D_{ij}(\mathbf{u})) + (\mathbf{u}\cdot\nabla)\,u_i + (\nabla p)_i = f_i \qquad 1 \leqslant i \leqslant 2 \tag{2.1}$$

$$\nabla\cdot\mathbf{u} = 0, \tag{2.2}$$

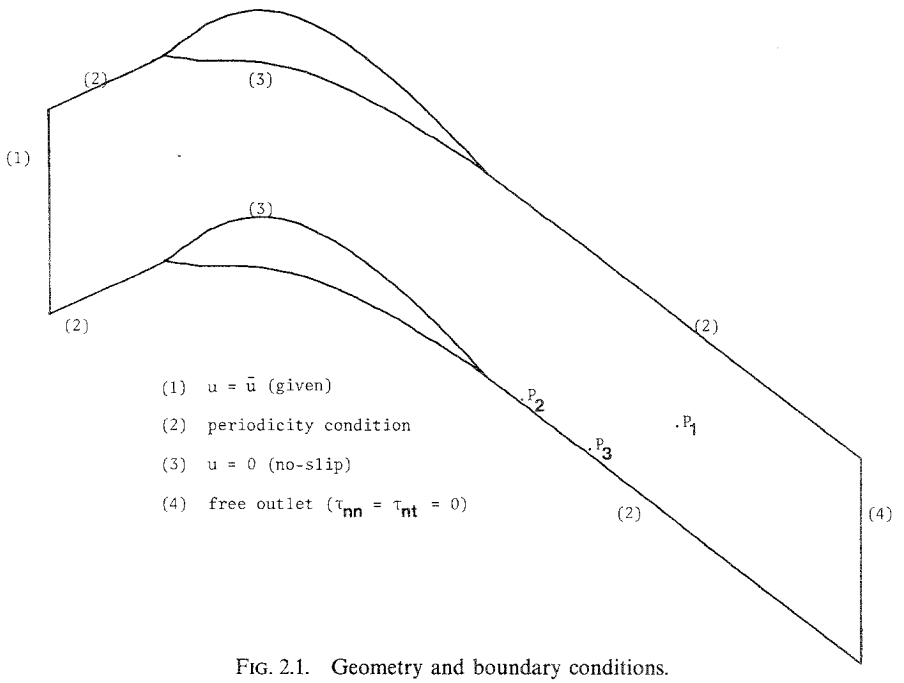

FIG. 2.1. Geometry and boundary conditions.

where $\mathbf{u} = (u_1, u_2)$ is the velocity field, p is the pressure, and

$$D_{ij}(\mathbf{u}) = \tfrac{1}{2}(\partial u_i/\partial x_j + \partial u_j/\partial x_i). \tag{2.3}$$

Equations (2.1) and (2.2) must be solved in a domain Ω along with appropriate initial and boundary conditions described in Fig. 2.1.

This is known as a cascade flow: periodicity conditions mean that this can be thought of as a section of a circular turbine.

We first consider a steady-state problem and discretize the system (2.1) by a standard Galerkin formulation and a standard finite element approximation. The domain is divided into quadrilaterals, velocity is interpolated by a full biquadratic approximation and pressure is taken piecewise linear and discontinuous (see Fig. 2.2). This element can be shown to be second order accurate and to satisfy the inf-sup stability condition of Brezzi [4] and Babuska [5] (cf. Fortin, [6] for a dis-

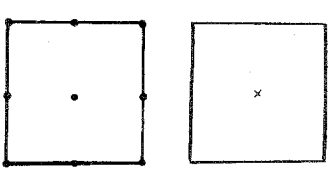

FIG. 2.2. The element used: (·) velocity degrees of freedom (u_1, u_2), (×) Pressure degrees of freedom (p, $\partial p/\partial x$, $\partial p/\partial y$).

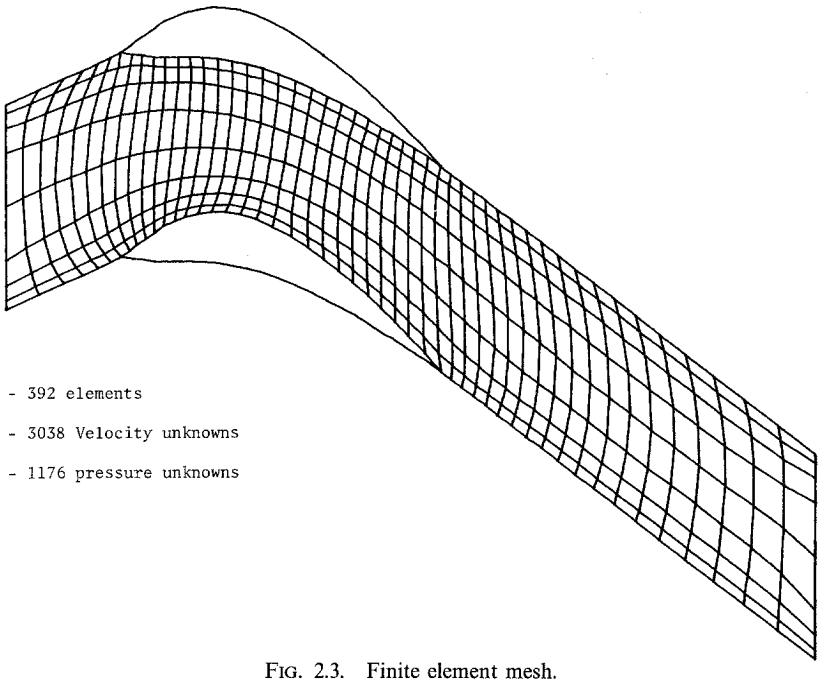

FIG. 2.3. Finite element mesh.

cussion of related elements). This choice of element was made from the experimental evidence that it is one of the best two-dimensional elements on a cost–accuracy scale.

We, moreover, used the trick of Fortin–Fortin [7] to eliminate internal nodes. The mesh used (Fig. 2.3) was based on a 8×49 partition of the blade-to-blade region.

When a time-dependent problem was solved, we used a Gear's scheme based on the approximation

$$\partial \mathbf{u}/\partial t = (3\mathbf{u}^{n+1} - 4\mathbf{u}^n + \mathbf{u}^{n-1})/2\,\Delta t + \theta(\Delta t^2). \tag{2.4}$$

This second order accurate two-step method is known to be stiff stable. It yields an implicit scheme: at each time step a non-linear problem has to be solved. We used a variant of Newton's method described in Fortin–Fortin [8] which marries a standard Newton–Raphson technique with a Uzawa's iteration (cf. Fortin–Glowinski [21]) for the incompressibility constraint. Moreover, in order to reduce computational cost, the matrix in Newton's method was kept fixed as long as the method converged in less than 5 iterations for each time step. Whenever this limit was exceeded, the matrix was updated and refactorized. The total result was a robust and stable solution scheme that provided a quite reasonable approximation of the Navier–Stokes equations in the present state of the art (although a finer mesh would of course be preferable).

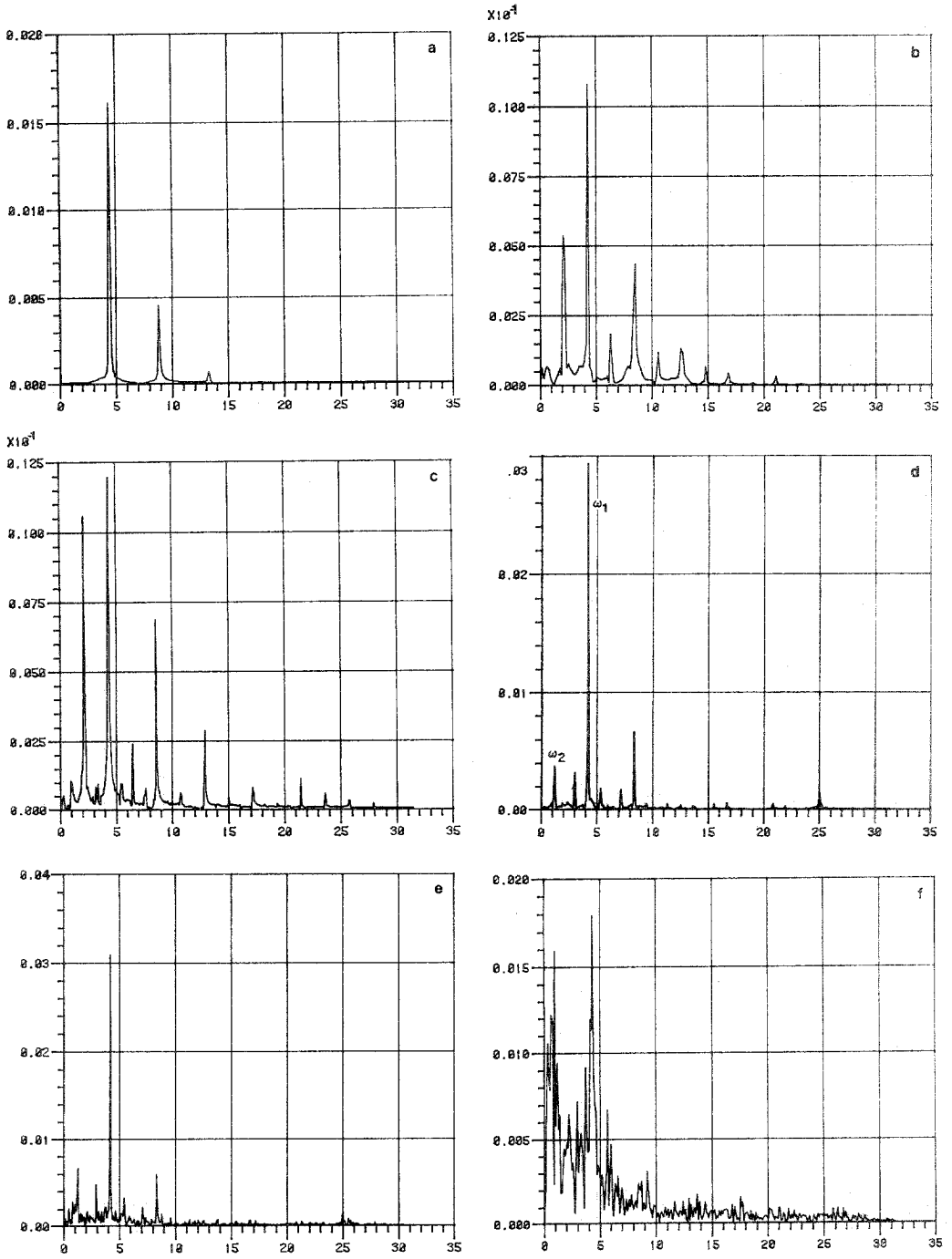

FIG. 3.1. Amplitude vs frequency. (a) Re = 1200, (b) Re = 1700, (c) Re = 1900, (d) Re = 2000, (e) Re = 2100, (f) Re = 2200.

3. Description of the Experiment

Having realised that in the problem at hand it was impossible to get a steady-state solution for a Reynolds number larger than about 600, even with a careful loading procedure, it was quite natural, from general knowledge of fluid behavior, to think that a bifurcation could have occurred towards an unsteady, probably periodic, solution. Starting the time-dependent code from the last steady solution and increasing the Reynolds number, it was soon observed that a Karman vortex street had indeed developed behind the turbine blade. A Fourier analysis of a sampling of the velocity at a few points indeed showed a perfect periodic pattern (Fig. 3.1a). Increasing the Reynolds number by small steps (≈ 50), the next phenomenon to occur was a period doubling at about $\mathrm{Re} = 1700$ (Fig. 3.1b). A sequence of period doublings being a feature on the route to chaos, one could wonder whether or not other period doublings would be observed, presumably following Feigenbaum's law [9]

$$(\mathrm{Re}_{n+1} - \mathrm{Re}_n)/(\mathrm{Re}_{n+2} - \mathrm{Re}_{n+1}) \approx 4.6692016, \tag{3.1}$$

at least approximately. Indeed around Reynolds number 1900, a second period doubling can be observed in the spectrum (Fig. 3.1c). It is, however, weak and a further increase makes the whole pattern disappear. At $\mathrm{Re} = 2000$, one observes rather the appearance of two independent frequencies (Fig. (3.1d) well characterized by beats. Finally at $\mathrm{Re} = 2200$, the spectrum can be thought of as continuous, even if a fundamental frequency is still apparent (Fig. 3.1f).

Two explanations can be advanced for this phenomenon. It is possible that chaos could be obtained through successive period doublings but that the resulting periodic solutions are becoming less and less attractive and that our system jumped to the basin of another attractor (e.g., a two-dimensional torus) and followed then another branch of bifurcations. Such a jump could have been triggered by a change in time step that was made in order to keep the convergence of our Newton's method fast enough. Another possible explanation is that varying the time step indeed changed our system to a two-parameter system and in such systems many competing scenarios leading to chaos are possible (cf. Holmes [16]). It must be noted that both period doubling or multiple frequencies are observed in experimental situations (cf. Gollub–Benson–Steinman [2], Ruelle [1]).

4. Phase Diagrams, Dimension Calculation, and Lyapunov's Exponents

Other insights can be obtained from visualization of the flow. Streamlines indeed show a modification of the flow (Fig. 4.1). Although one still observed a vortex shedding at $\mathrm{Re} = 2200$, it is now irregular in the size of the vortices and the delay between their appearance. But the most informative figures are phase portraits. They are computed by mapping values of the velocity at the same point but

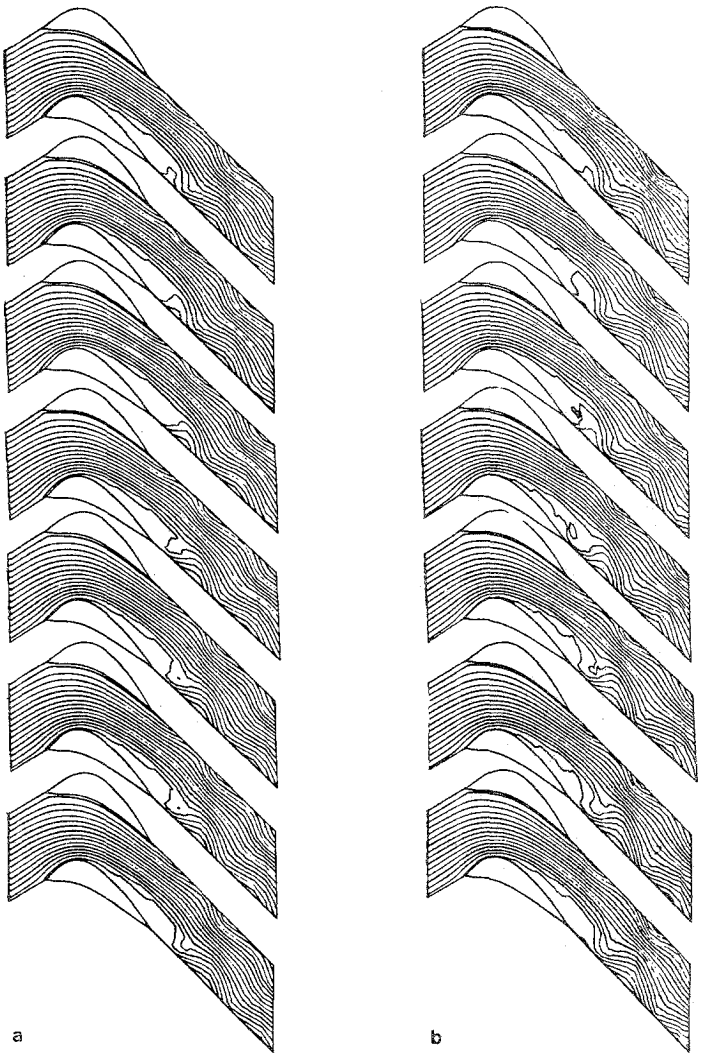

FIG. 4.1. Streamlines over one period. (a) Re = 1700, (b) Re = 2200.

separated by multiples of a fundamental delay T, that is, by forming vectors of the form

$$(V(t),\ V(t+T),\ V(t+2T),\ldots,\ V(t+(m-1)\ T)) = B_m(t) \tag{4.1}$$

in an m-dimensional space.

One can expect (Takens [10]) $B_m(t)$ to possess the same properties as the dynamical system with N variables for m large enough. Indeed, for $m \geqslant 2N+1$, this gives generically an embedding of the phase space of the dynamical system into this

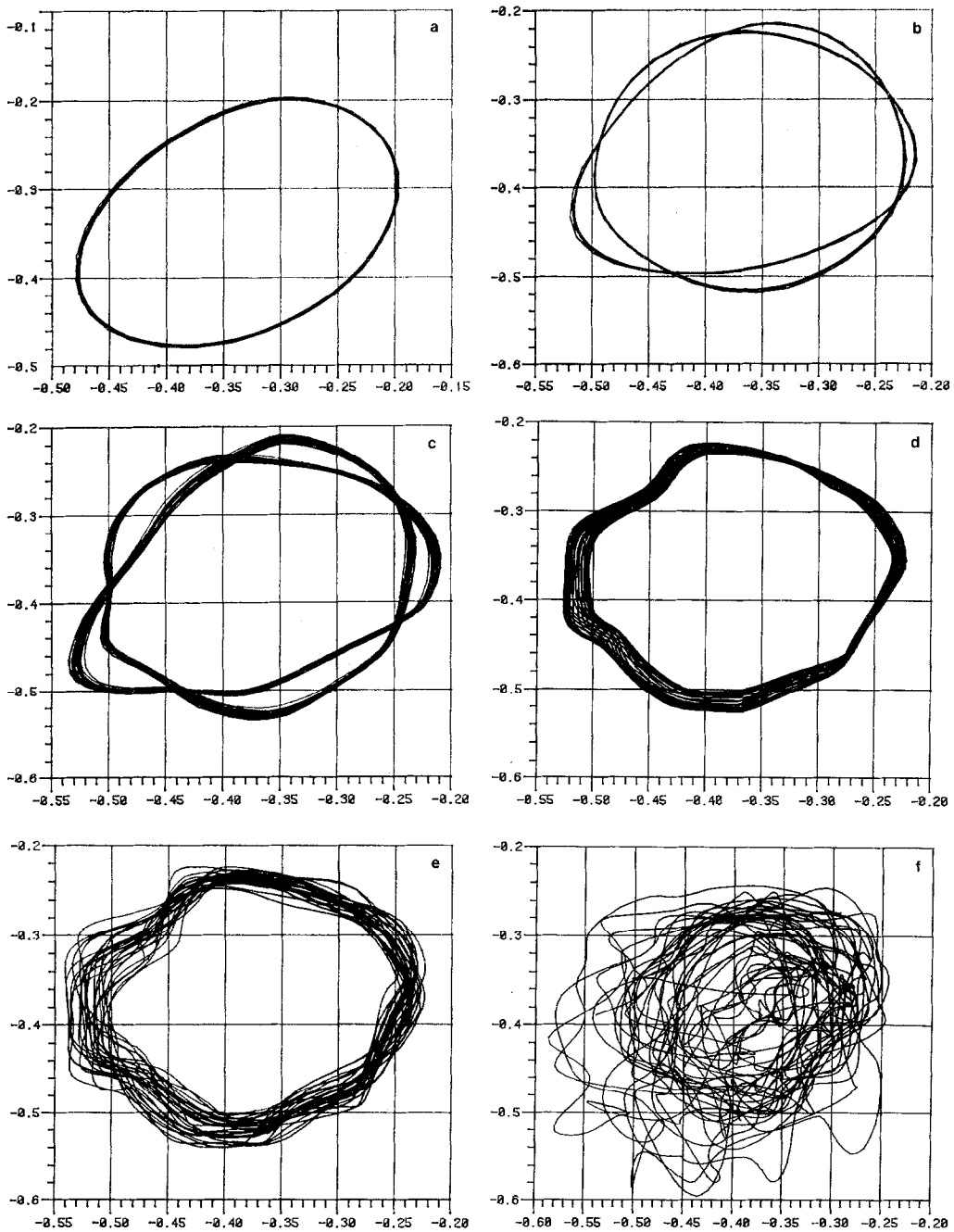

FIG. 4.2. Phase diagrams ($m=2$), ($V(t+T)$ vs $V(t)$ ($T=0.575$)) at point P_1: (a) Re = 1200, (b) Re = 1700, (c) Re = 1900, (d) Re = 2000, (e) Re = 2100, (f) Re = 2200; at point P_2: (g) Re = 1200, (h) Re = 2000, (i) Re = 2200; at point P_3: (j) Re = 1200, (k) Re = 2000, (l) Re = 2200.

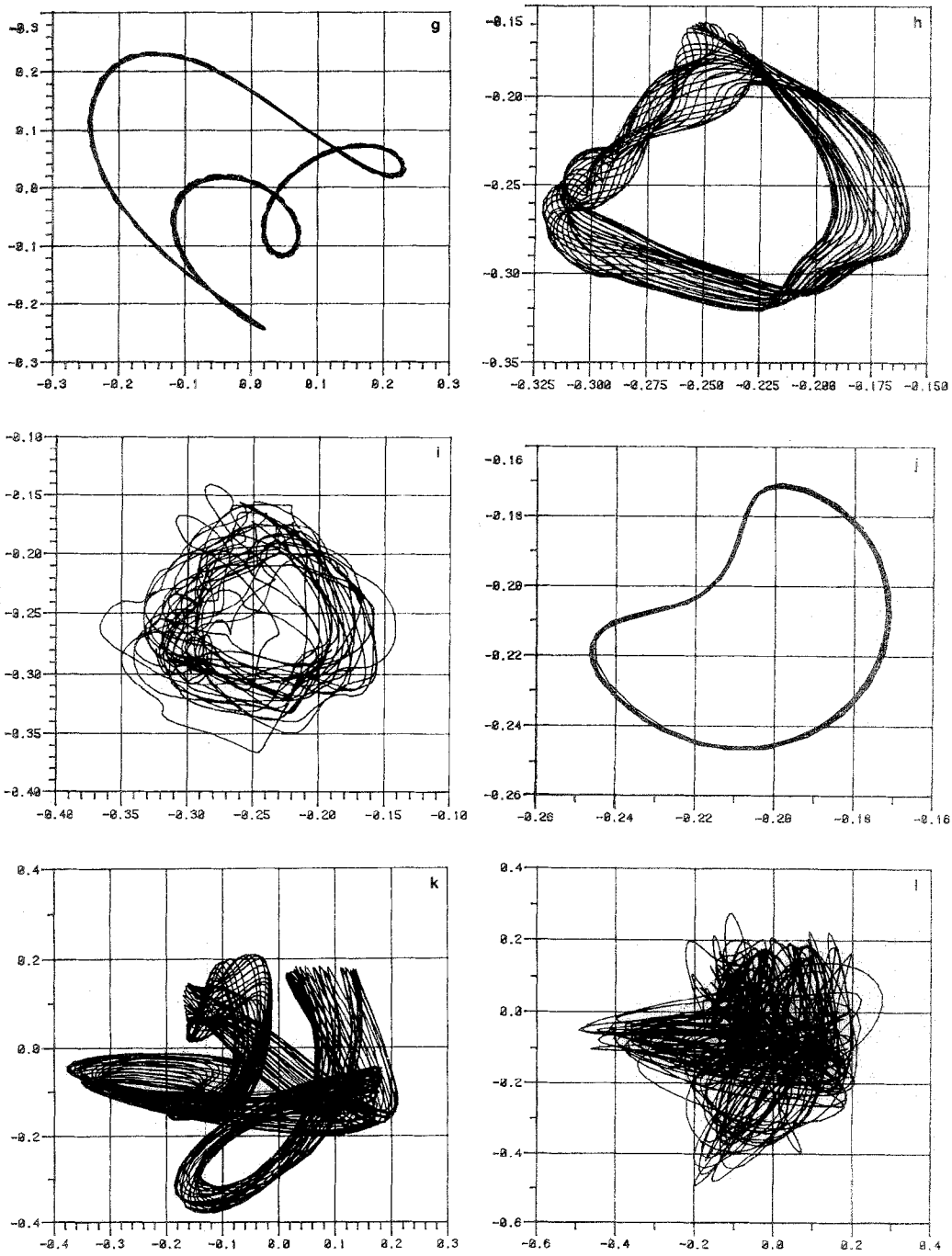

FIGURE 4.2—*Continued.*

m-dimensional space. However, one may expect to obtain valuable information for a much smaller m. The choice of T is arbitrary. However, if the phenomenon under study is periodic (with period τ), then T must be different from τ since in that case, the phase diagram would be compressed on the diagonal. A good approximation for T is $\tau/4$ but this choice must be ajusted by trial and error to give the best representation.

Figure 4.2 presents phase diagrams for $m = 2$ for different values of the Reynolds number and at different sampling points P_1, P_2, and P_3 (see Fig. 2.1). These diagrams clearly follow the results of the Fourier analysis. For $\mathrm{Re} = 1200$, the simple loop corresponds to a simple periodic motion. Period doubling ($\mathrm{Re} = 1700$) indeed produces a doubling of the curve, while the second (weak) period-doubling at $\mathrm{Re} = 1900$ again makes a second separation appear, this time hardly distinguishable with respect to noise. Results for $\mathrm{Re} = 2000$ introduce a drastic change, the diagram clearly looks like a two-dimensional strip embedded in a higher dimensional space. For $\mathrm{Re} = 2100$, this begins to lose sharpness and at $\mathrm{Re} = 2200$, we have a clearly "chaotic" behavior possibly over an underlying average periodicity.

Another interesting way to characterize the flow consists in computing the dimensions of the attractors whose two-dimensional projection are depicted in the previous figure. There exists many definitions of dimension more or less related to the Hausdorff dimension. Let us recall that if we have a bounded subset of a p-dimensional euclidian space R^p, then

$$d_H = \lim_{\varepsilon \to 0} \frac{\log(N_p(\varepsilon))}{\log(\varepsilon)}, \tag{4.2}$$

where $N_p(\varepsilon)$ is the minimum number of p-dimensional boxes of side ε required to cover the set. It should be noted that the dimension defined above is usually referred to as the capacity of a set but it seems that the Hausdorff dimension and the capacity are the same for attractors (see Grassberger–Procaccia [11]). From a practical standpoint, Eq. (4.2) becomes rapidly useless due to the formidable amount of computation involved when p is large and ε small (cf. Greenside–Wolf–Swift–Pignataro [12]). Consequently other dimension definitions have been proposed to overcome the numerical impracticality of Definition 4.2. We have adopted what is called the correlation dimension (cf. Grassberger–Procaccia [13]) defined as

$$d_c = \lim_{\varepsilon \to 0} \frac{\log(C_p(\varepsilon))}{\log \varepsilon}, \tag{4.3}$$

where $C_p(\varepsilon)$ is the number of pairs of data points whose separation in phase space is less than ε, divided by N^2. That is,

$$C_p(\varepsilon) = \lim_{N \to \infty} \frac{1}{N^2} \sum_{\substack{i,j=1 \\ i \neq j}}^{N} \theta(\varepsilon - |\bar{X}_i - \bar{X}_j|), \tag{4.4}$$

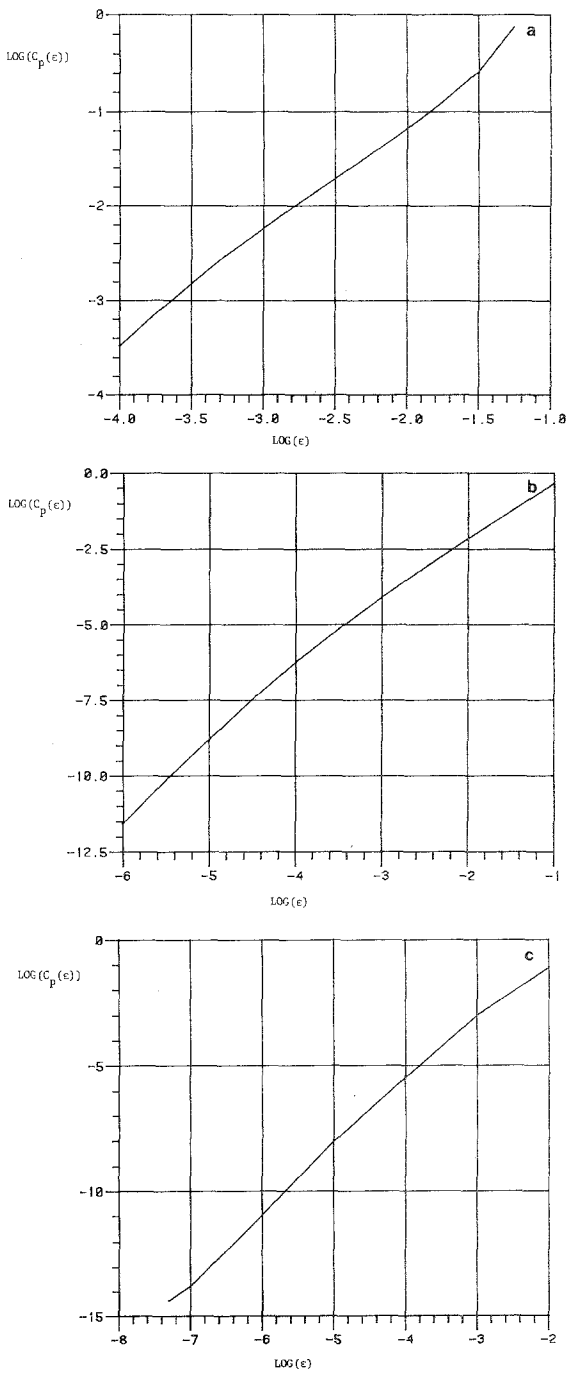

FIG. 4.3. Dimension computation (Log $C_p(\varepsilon)$ vs Log ε). (a) Re = 1700 (slope ≈ 1.16), (b) Re = 2000 (slope ≈ 2.23), (c) Re = 2200 (slope ≈ 2.57).

where θ is the Heaviside function, $\bar{X}_i$ and $\bar{X}_j$ a pair of data points in the phase space of dimension p, and N the total number of data points. It has been shown [13] that (4.3) and (4.2) give very similar results when both are applicable. To obtain the correlation dimension, one has first to fix a value for the phase-space dimension p ($p=2$, e.g.), compute $C(\varepsilon)$ for different values of ε, plot the graph of $\log(C(\varepsilon))$ versus $\log(\varepsilon)$ and determine the slope of that curve (by a least square method, e.g.). This algorithm is then repeated with an increased value of p until the slope of the curve becomes independent of p.

The phase-space diagrams (Fig. 4.2) lead us to think that the dimension of the attractors should be one up to $\mathrm{Re}=2000$, where it must be around two. For $\mathrm{Re}=2200$ the apparently chaotic behavior should correspond to a fractal dimension. The results, shown in Fig. 4.3, are not as clear as could be hoped but nevertheless agree with intuition. The difficulties arise of course from the large number of points necessary to estimate the dimension. The 8000 points we used are indeed a small number compared to the 20,000 normally used for similar computation. It must be recalled that each of these points requires the solution of the full non-linear Navier–Stokes equations and consequently this number was the maximum we could afford. The conclusion from this calculation is that at $\mathrm{Re}=2200$, the dimension of the attractor is around 2.57 and is surely strictly larger than 2 and smaller than 3. We thus have an attractor of fractal dimension. The last question was whether this attractor was indeed strange or in fact chaotic (in the sense of Gregobi *et al.* [17]). The criterion for "chaoticity" is the existence of a positive Lyapunov exponent. Let us recall briefly the definition of a Lyapunov exponent (see Farmer [14]).

Let us consider an infinitesimal ball that has radius $\varepsilon(0)$ at $t=0$ and located in the basin of attraction of the attractor. As time goes on, the ball will distort but since ε is very small, the change in shape is determined only by the linear part of the flow, and thus the ball remains ellipsoid. We thus define the Lyapunov exponents

$$\lambda_i = \lim_{t\to\infty} \lim_{\varepsilon(0)\to 0} (1/t)\log(\varepsilon_i(t)/\varepsilon(0)), \qquad 1\leqslant i\leqslant p, \tag{4.5}$$

where the $\varepsilon_i(t)$ are the principal axes of this ellipsoid. A more intuitive insight is obtained by replacing (4.5) by

$$\varepsilon_i(t) \approx \varepsilon(0)\, e^{\lambda_i t}, \qquad 1\leqslant i\leqslant p, \tag{4.6}$$

when t is large and $\varepsilon(0)$ small. It is usually accepted as a definition that strange attractors are characterized by (at least) one positive Lyapunov exponent, expressing an exponential divergence of two nearby trajectories in that direction. Since the attractor is bounded, this exponential divergence implies a systematic folding process generally giving rise to a set of fractal dimension.

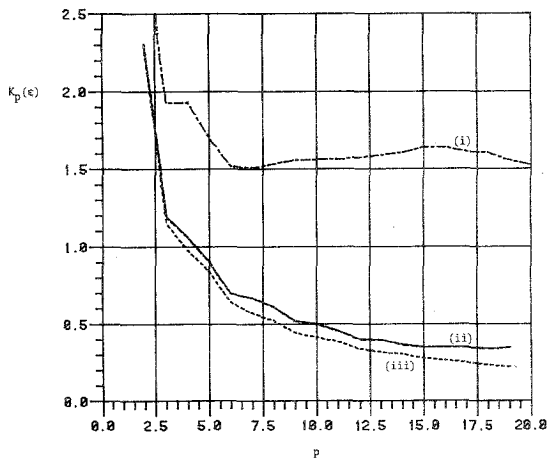

FIG. 4.4. $K_p(\varepsilon)$ vs p ($\varepsilon = 0.02$). (i) Re = 2200, (ii) Re = 2000, (iii) Re = 1200.

However, it is difficult to compute directly the Lyapunov exponents. Fortunately, Grassberger and Procaccia [15] have shown that the quantity

$$K_2 = \lim_{\substack{p \to \infty \\ \varepsilon \to 0}} \frac{1}{T} \log(C_p(\varepsilon)) - \log(C_{p+1}(\varepsilon)) = \lim_{\substack{p \to \infty \\ \varepsilon \to 0}} K_p(\varepsilon) \tag{4.7}$$

is a lower bound for the sum of positive Lyapounov exponents (T defined in (4.1)). Figure 4.4 displays the evolution of $K_p(\varepsilon)$ with respect to p. For Re = 1200 and Re = 2000, the curve clearly converges towards 0. For Re = 2200, the curve reaches a lower bound around 1.5 showing that at least one Lyapunov exponent is positive and that the attractor is indeed strange.

5. CONCLUSION

This numerical experiment seems to confirm a few theoretical results and also some conjectures concerning the relation between bifurcation theory, strange attractors, and fluid flow problems. Indeed, we have shown that an attractor of fractal dimension was present in our problem confirming the results of Teman–Foias [3] who gave a theoretical upper bound for this attractor. We have also established a link between bifurcation theory and fluid mechanics problems by showing that results from more or less elementary bifurcation problems are also valid for complex models such as the Navier–Stokes equations. The question of course arises whether the phenomena we present are really related to fluid mechanics: they could be merely artifacts of the numerical approximation and disappear for smaller mesh-

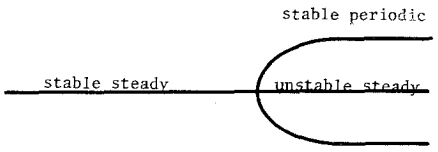

FIG. 5.1. Hopf bifurcation diagram.

size. The cost of a computation on a much smaller mesh does not enable us to give a definitive answer now. Some facts, however, lead us to think that the transition described is at least qualitatively correct (but might not be the only one possible):

(i) The computed flow is realistic and in fact very weakly chaotic.

(ii) A similar study, using spectral methods on a purely academic problem, has been performed by Lafon [18]. Although the problems and the numerical methods are totally different, the results obtained are strikingly close. This permits us to think that the phenomena observed are indeed related to the Navier–Stokes equations themselves and not to a numerical procedure. This study of Lafon also shows that the periodic component still visible in the spectrum at $Re = 2200$ is likely to disappear for higher Reynolds number and that a fully developed chaos will ultimately appear.

(iii) The route to chaos that we observed seems to be quite generic. The reader should compare the spectra of Fig. 3.1 with those of Ref. [20], which come from experimental study of a chemical reaction. Some are close enough to be interchanged.

From a mathematical point of view, the effect of mesh size on bifurcation results can be seen as a perturbation by a second parameter. It must be emphasized that a Hopf bifurcation (Fig. 5.1) is generically stable under such a perturbation in the sense that it will not be changed to another type of diagram (cf. Chaps. VI and VIII of [22] and Sect. 4 of [23]). This stability does not hold in a pitchfork bifurcation of steady solutions (Fig. 5.2a) where the perturbed diagram may even contain limit points (Figs. 5.2b and c) (cf. Chap. III of [22]). Following discretized branches of steady solutions may thus make spurious solutions appear. Unsteady solutions are likely to meet and follow the physically expected transition to a periodic solution.

Finally, many questions arise from this work. For example, one may wonder whether or not it is possible to recover useful information from the computed chaotic flow, for instance, drag coefficients or some other engineering quantity. Another interesting idea would be to compare the chaos obtained with the hypothesis of standard turbulence models, in particular with respect to isotropy. In order to pursue these goals we are now studying the possibility of doing the same kind of experiment on a geometry where experimental data are available for comparison.

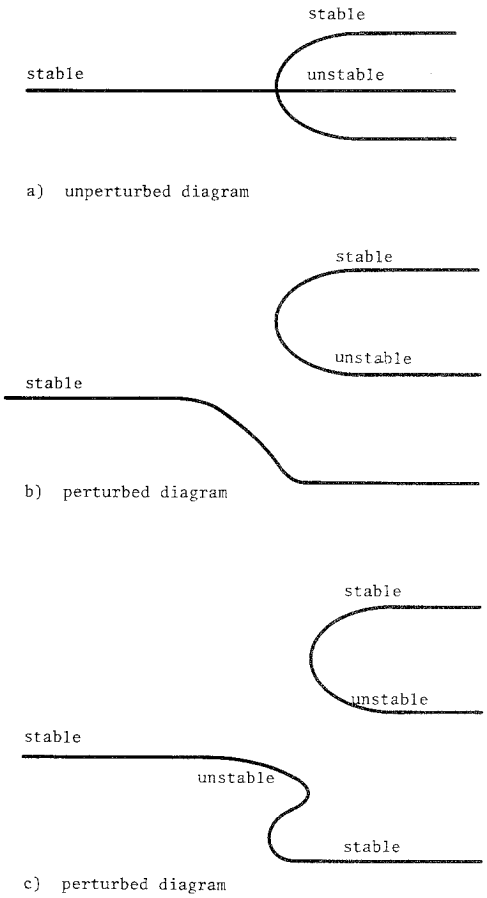

FIG. 5.2. (a) Unperturbed diagram, (b) perturbed diagram, (c) perturbed diagram.

REFERENCES

1. D. RUELLE, *Math. Intelligencer* **2**, 126 (1980).
2. J. P. GOLLUB, S. V. BENSON, AND J. STEINMAN, *Ann. New York Acad. Sci.* **357**, 22 (1979).
3. P. CONSTANTIN, C. FOIAS, O. P. MANLEY, AND R. TEMAM, *J. Fluid Mech.* **150**, 427 (1985).
4. F. BREZZI, *RAIRO*, **8**, No. R2, 129 (1981).
5. I. BABUSKA, *Numer. Math.* **16**, 322 (1971).
6. M. FORTIN, *Int. J. Numer. Methods Fluids* **1**, 347 (1981).
7. M. FORTIN AND A. FORTIN, *Int. J. Numer. Methods Fluids* **5**, No. 10, 911 (1985).
8. M. FORTIN AND A. FORTIN, *Commun. Appl. Numer. Methods* **1** No. 5, 205 (1985).
9. M. J. FEIGENBAUM, *J. Stat. Phys.* **19**, 25 (1978).
10. F. TAKENS, *Lecture Notes in Mathematics*, Edited by D. A. Rand and L. S. Young (Springer-Verlag 1981), p. 431.
11. P. GRASSBERGER AND I. PROCACCIA, *Physica D* **9**, 189 (1983).

12. H. S. GREENSIDE, A. WOLF, J. SWIFT AND T. PIGNATARO, *Phys. Rev. A* **25**, No. 6, 3453 (1982).
13. P. GRASSBERGER, AND I. PROCACCIA, *Phys. Rev. Lett.* **50**, No. 5, 346 (1983).
14. J. D. FARMER, *Physica D* **4**, 366 (1982).
15. P. GRASSBERGER AND I. PROCACCIA, *Phys. Rev. A***28**, No. 4, 2591 (1983).
16. P. HOLMES, *Phys. Lett., A* **104**, 299 (1984).
17. C. GREGOBI, E. OTT, S. PELIKAN, AND J. A. YORKE, *Physica D***13**, 261 (1984).
18. A. LAFON, Etude des attracteurs pour des écoulements bidimensionnels de fluides visqueux incompressibles, Thèse de Doctorat, Université de Paris VI, 1985 (unpublished).
19. R. TEMAM, "Navier–Stokes Equations and Non-linear Functional Analysis," CBMS-NSF Regional Conference Series in Applied Mathematics (SIAM, Philadelphia, 1983) Vol. 41.
20. C. VIDAL, J.-C. ROUX, S. BACHELART, AND A. ROSSI, *Ann. New York Acad. Sci.* **357**, 377 (1979).
21. M. FORTIN AND R. GLOWINSKI, *Résolution numérique de problèmes aux limites par des méthodes de lagrangien augmenté* (Dunod, Paris, 1982).
22. M. GOLUBITSKY AND D. G. SCHAEFFER, *Singularities and Groups in Bifurcation Theory* (Springer-Verlag, Berlin, 1985), Vol. 1.
23. F. BREZZI, J. RAPPAZ, AND P. A. RAVIART, *Numer. Math.* **38**, 1 (1981).